JACS
JOURNAL OF THE AMERICAN CHEMICAL SOCIETY

Communication

pubs.acs.org/JACS

Rare Examples of Fe(IV) Alkyl-Imide Migratory Insertions: Impact of Fe—C Covalency in $(Me_2IPr)Fe(=NAd)R_2$ (R = ^{neo}Pe, 1-nor)

Brian P. Jacobs,[†] Peter T. Wolczanski,*[,†] Quan Jiang,[‡] Thomas R. Cundari,*[,‡] and Samantha N. MacMillan[†]

[†]Department of Chemistry & Chemical Biology, Baker Laboratory, Cornell University, Ithaca, New York 14853, United States
[‡]Department of Chemistry, CASCaM, University of North Texas, Denton, Texas 76201, United States

Supporting Information

ABSTRACT: The iron(IV) imide complexes, $(Me_2IPr)R_2Fe{=}NAd$ (R = ^{neo}Pe (**3a**), 1-nor (**3b**)) undergo migratory insertion to iron(II) amides $(Me_2IPr)RFe\{NR(Ad)\}$ (R = ^{neo}Pe (**4a**), 1-nor (**4b**)) without evidence of imidyl or free nitrene character. By increasing the field strength about iron, odd-electron reactivity was circumvented via increased covalency.

Recent investigations of iron imido complexes[1] feature species exhibiting imidyl (nitrogen radical, $RN^{\bullet-}$) reactivity in the context of carbon−hydrogen bond activation,[2−7] to remarkably stable high oxidation state species.[8−12] The imidyl, "nitrene-insertion" reactivity, such as that described by Betley,[2] can be construed as a rebound process in which hydrogen atom transfer (HAT) is followed by coupling of carbon- and nitrogen-based radicals. Aziridinations[2−7,13] often accompany or appear related to HAT initiated reactions, and can be considered as complementary, stepwise radical additions to olefins.

Classical imido (RN^{2-}) complexes are often unreactive, but in combination with electrophilic (d^0) early transition metal sites, can activate aliphatic CH bonds, including that of CH_4, in a clear concerted fashion.[14,15] Can iron complexes also exhibit such behavior? The covalency of related Fe(IV) imides must be extremely high in order to attenuate imidyl character, and strong field ligands such as alkyls and N-heterocyclic carbenes are attractive ancillary ligands.[16,17] Herein are described formally Fe(IV) imido complexes that exhibit migratory insertion behavior best construed as concerted. The reactions are rare examples of $L_mM^n(=X)R \rightarrow L_mM^{(n-2)}{-}X{-}R$ (X = O,[17] NR′[18−20]) insertions that incur a formal oxidation state change, and portend the possibility of reactions such as olefin metathesis with first-row transition metal systems.

A variety of pseudotetrahedral $L_nFe(^{neo}Pe)_2$ complexes were targeted to avoid β-H-elimination paths, and synthesized via metathetical procedures[21−27] from corresponding halides. Upon treatment with various oxidants, including azides,[28] 2,2,5,5-tetramethylhexane was detected with few exceptions. Exposure of $(tmeda)Fe(^{neo}Pe)_2$ (**1**, S = 2, Scheme 1) to AdN_3 (Ad = 1-adamantyl) afforded AdN = CH^{t}Bu, and no R−R coupling, suggestive of a nitrene insertion process.

To generate a strong field, three-coordinate environment likely to induce imide formation, bulky Me_2IPr[26−29] was utilized as an ancillary ligand. 1-Norbornyl (1-nor) was another featured alkyl, as β-H-elimination is obviated by the formation of bridgehead olefins, and there is a history of 1-nor providing exceptionally strong fields,[30] as in $Fe(1\text{-nor})_4$.[23,31,32]

Scheme 1. Syntheses of L_nFeR_2

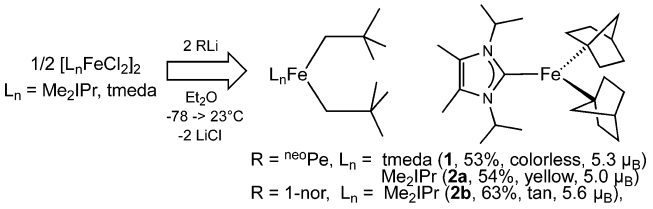

$(Me_2IPr)Fe(^{neo}Pe)_2$ (**2a**) and $(Me_2IPr)Fe(1\text{-nor})_2$ (**2b**) were prepared from metathesis of $[(Me_2IPr)FeCl_2]_2$ with ^{neo}PeLi and (1-nor)Li, respectively (Scheme 1) and possess μ_{eff} values of 5.0 (**2a**) and 5.6 μ_B (**2b**),[33] indicative of S = 2 centers. A molecular view of **2b** is given in Figure 1, along with core

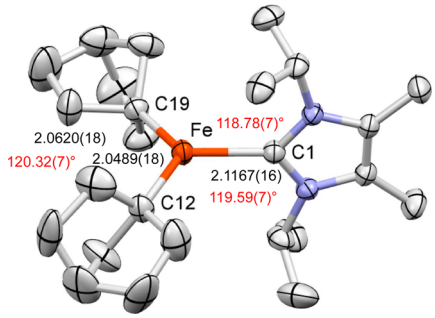

Figure 1. Molecular view of $(Me_2IPr)Fe(1\text{-nor})_2$ (**2b**); selected bond distances (black, Å) and angles (red) are given.

interatomic distances and angles. Three-coordinate **2b** is nearly trigonal despite the steric bulk of the tertiary 1-norbornyl substituents. A similar geometry is observed for $(Me_2IPr)Fe(^{neo}Pe)_2$ (**2a**, X-ray) but severe twinning problems hampered refinement.

Exposure of $(Me_2IPr)Fe(^{neo}Pe)_2$ (**2a**) to AdN_3 afforded a persistent dark green solution at −78 °C that slowly became yellow at 23 °C. ^{1}H NMR spectroscopy, protic quenching studies that yielded $AdNH(^{neo}Pe)$, and X-ray crystallography

Received: July 4, 2017
Published: August 10, 2017

DOI: 10.1021/jacs.7b06960
J. Am. Chem. Soc. 2017, 139, 12145−12148

revealed the migratory insertion product, $(Me_2IPr)Fe\{N(Ad)^{neo}Pe\}(^{neo}Pe)$ (**4a**, 65%), as shown in Scheme 2. Its μ_{eff} of 5.1 μ_B[33] was consistent with an $S = 2$ ferrous center.

Scheme 2. $(Me_2IPr)Fe(=NAd)R_2$ to $(Me_2IPr)Fe\{N(Ad)R\}R$ ($R = {}^{neo}Pe$, 3a → 4a; 1-nor, 3b → 4b)

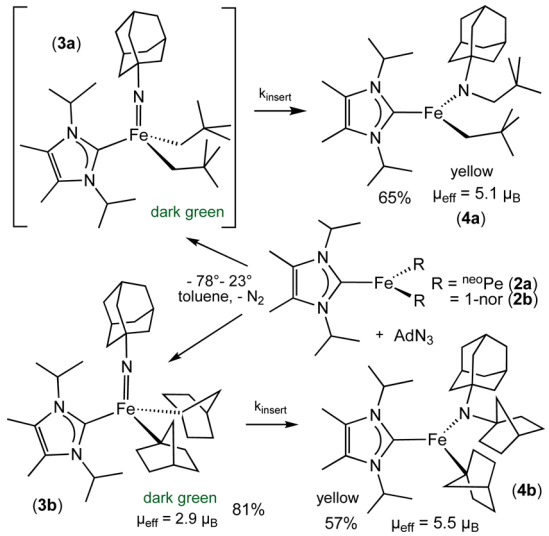

Figure 2 illustrates a molecular view of $(Me_2IPr)Fe\{N(Ad)^{neo}Pe\}(^{neo}Pe)$ (**4a**), which exhibits a slightly distorted trigonal structure with the Me_2IPr ligand again vertical to the trigonal plane. Core bond distances are normal for a low coordinate high spin ferrous center, and the d(FeC) for the neopentyl ligand is ∼0.07 Å shorter than the corresponding NHC interaction.

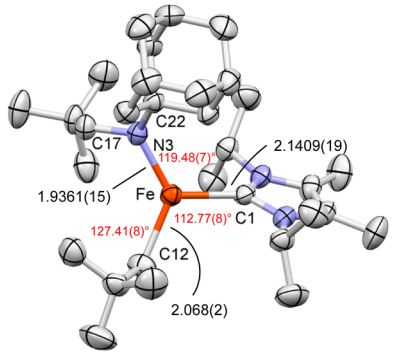

Figure 2. View of $(Me_2IPr)Fe\{N(Ad)^{neo}Pe\}(^{neo}Pe)$ (**4a**); selected bond distances (black, Å) and angles (red) are given.

Failure to isolate dark green **3a** prompted a switch to $(Me_2IPr)Fe(1\text{-nor})_2$ (**2b**).[23,31,32] Treatment of **2b** with AdN_3 under identical conditions permitted isolation of dark green $(Me_2IPr)Fe(=NAd)(1\text{-nor})_2$ (**3b**, 81%), and its μ_{eff} of 2.9 μ_B[33] revealed an intermediate spin ($S = 1$) system. Imide **3b** was thermally converted to the yellow insertion product, $(Me_2IPr)Fe\{N(Ad)(1\text{-nor})\}(1\text{-nor})$ (**4b**, 57%, $S = 2$, $\mu_{eff} = 5.5$ μ_B), and protic quenching of **4b** provided AdNH(1-nor). Spectroscopic characteristics relating **3b** to **3a** suggested the latter to be the thermally unstable imide, $(Me_2IPr)Fe(=NAd)(^{neo}Pe)_2$ (**3a**).

Figure 3 shows the distorted tetrahedral structure of $(Me_2IPr)Fe(=NAd)(1\text{-nor})_2$ (**3b**), highlighting its short (1.6723(18) Å), nearly linear (168.04(15°)) iron imide linkage.

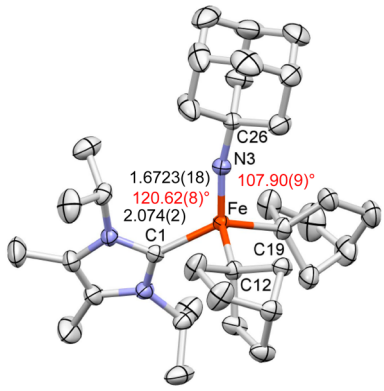

Figure 3. Molecular view of $(Me_2IPr)Fe(=NAd)(1\text{-nor})_2$ (**3b**). Selected bond distances (black, Å) and angles (red, deg): Fe−C12, 2.005(2); Fe−C19, 2.024(2); N3−C26, 1.437(3); N3−Fe−C12, 105.09(9); C12−Fe−C19, 103.77(9); C1−Fe−C12, 96.98(8); C1−Fe−C19, 119.23(9); Fe−N3−C26, 168.04(15).

The distorted core appears to reflect steric interactions, as the adamantyl unit is tipped away from the ^{i}Pr group on the Me_2IPr, although the 1-nor ligands span a C12−Fe−C19 angle of only 103.77(9)°. Favorable dispersion forces, specifically in Fe(IV) complexes, appear to play a role in stabilization of hindered systems.[23,34]

Calculations (B3PW91-GD3/6-31+G(d)) of $(Me_2IPr)Fe(=NAd)(1\text{-nor})_2$ (**3b**) confirm an $S = 1$ ground state. There is an impressive admixture of 1-nor and Me_2IPr character to the Fe($d\pi$)−N($p\pi$)frontier orbitals of **3b** (6 α- and 4 β-orbitals span 0.10 eV), such that correlating spins and defining a ligand field (d^n) are subjective. The significant amounts of iron and carbon character are consistent with strong covalent interactions that belie the formal Fe(IV) oxidation state.[35]

MCSCF calculations were conducted at the DFT-optimized geometry of **3a**. Within the CAS(14,14) active space, MCSCF natural orbitals show significant delocalization, particularly four nearly doubly occupied (natural orbital population ∼1.9 e^-) orbitals with mixed FeC(σ), (^{neo}Pe), and FeN(π) character (Figure 4a.). Next highest in energy are two singly occupied

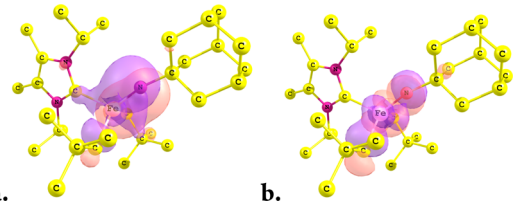

Figure 4. CAS(14,14) natural orbitals of **3a** (contour value = 0.03): (a) FeC(σ) (^{neo}Pe) with FeN(π); (b) FeN(π^*).

orbitals that are primarily Fe(3d) in character, followed by two natural orbitals (occupation ∼0.1 e^-) that are FeN(π^*) (Figure 4b.). The total Mulliken population of Fe among the 14 active space natural orbitals is 6.9 e^-,[35] implying significant covalency and charge delocalization among all iron-ligand bonds.

$(Me_2IPr)Fe(=NAd)(^{neo}Pe)_2$ (**3a**) could not be isolated, but it persisted in solution for a time sufficient to evaluate the insertion kinetics. $(Me_2IPr)Fe(=NAd)(1\text{-nor})_2$ (**3b**) could be similarly analyzed, and the results are listed in Table 1. The migratory insertion of **3a** to $(Me_2IPr)Fe\{N(Ad)^{neo}Pe\}(^{neo}Pe)$ (**4a**, $\Delta G^{\ddagger}(25°) = 20.4(8)$ kcal/mol) is ∼3.6 kcal/mol more favorable than the conversion of **3b** to $(Me_2IPr)Fe\{N(Ad)(1\text{-}$

DOI: 10.1021/jacs.7b06960
J. Am. Chem. Soc. 2017, 139, 12145−12148

Table 1. Migratory Insertion Rates of $(Me_2IPr)Fe(=NAd)R_2$ (R = ^{neo}Pe, 3a; 1-nor, 3b) to $(Me_2IPr)Fe\{N(R)Ad\}R_2$ (R = ^{neo}Pe, 4a; 1-nor, 4b)[a]

rxn	T (±1.0 °C)	k (s^{-1})	$\Delta G^{\ddagger}$
3a → **4a**[b]	−10.0	$4.85(8) \times 10^{-5}$	20.5(8)
3a → **4a**[b]	1.0	$2.84(29) \times 10^{-4}$	20.4(8)
3a → **4a**[b]	10.0	$1.17(8) \times 10^{-3}$	20.3(8)
3a → **4a**[b]	21.0	$4.78(30) \times 10^{-3}$	20.3(8)
3a → **4a**[b]	30.0	$1.37(8) \times 10^{-2}$	20.3(8)
3b → **4b**[c]	23.0	$4.85(8) \times 10^{-5}$	24.0(6)
3b → **4b**[c]	40.0	$2.84(29) \times 10^{-4}$	24.0(6)
3b → **4b**[c]	50.0	$1.17(8) \times 10^{-3}$	24.0(6)
3b → **4b**[c]	60.0	$4.78(30) \times 10^{-3}$	24.0(6)
3b → **4b**[c]	71.0	$1.37(8) \times 10^{-2}$	24.0(6)

[a]Toluene-d_8. [b][**3a**] = 0.057 M; $\Delta H^{\ddagger}$ = 22.3(8), $\Delta S^{\ddagger}$ = 6.5(1) eu. [c][**3b**] = 0.047 M; $\Delta H^{\ddagger}$ = 24.4(6), $\Delta S^{\ddagger}$ = 1.3(1) eu.

nor)})(1-nor) (**4b**, $\Delta G^{\ddagger}(25°)$ = 24.0(6) kcal/mol). Enthalpy ($\Delta\Delta H^{\ddagger} \sim 2.1$) and entropy ($\Delta\Delta S^{\ddagger} \sim 5.2$ eu) differences impart roughly the same changes in $\Delta\Delta G^{\ddagger}$.

Only additions of AdN_3 to **2e** and **3e** enabled spectroscopic observation of the Fe(IV) imide, but exposure of $R'N_3$ to various dialkyls $(Me_2IPr)FeR_2$ (R = ^{neo}Pe, **2a**; 1-nor, **2b**; mesityl (Mes)) enabled rough relative amide formation rates to be obtained: R = Mes ∼ ^{neo}Pe > 1-nor; R′ = Ph > $SiMe_3$ > Ad. In the presence of cyclohexene, 1,4-cyclohexadiene, or Et_3SiH, the **3b** to **4b** conversion was unaffected, and products from nitrene trapping were not observed. Slow alkyl exchanges are rampant, as **2a** and **2b** equilibrate with $(Me_2IPr)Fe(^{neo}Pe)$(1-nor) (**2ab**), **2b** and **4a** with $(Me_2IPr)Fe\{NAd(^{neo}Pe)\}$(1-nor) and **2ab**, and **4b** and **2a** with $(Me_2IPr)Fe\{NAd(1\text{-nor})\}(^{neo}Pe)$ and **2ab** in near statistical mixtures. Despite these complications, transiently generated **3a** provided **4a** when an equiv of **2b** was present, indicative of an intramolecular migratory insertion.

Calculations were conducted to gain insight into the reaction coordinate for insertion. Following the success of Power et al.,[34] B3PW91-GD3/6-31+G(d) simulations were applied to the migratory insertions. Figure 5 shows that the computations reproduce the lower barrier for **3a** → **4a** (R = ^{neo}Pe) over **3b** → **4b** (R = 1-nor): $\Delta\Delta G^{\ddagger}$(298 K) = 3.6 kcal/mol, $\Delta\Delta G^{\ddagger}$(calc) = 4.0 kcal/mol. The requisite spin-flip from the triplet imide surface to the quintet amide surface occurs prior to the transition state for insertion in both instances.

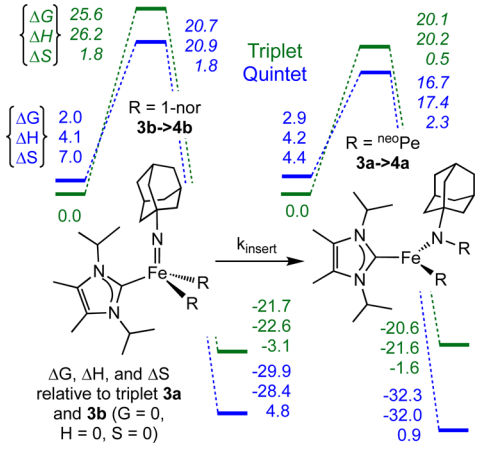

Figure 5. Triplet (green) and quintet (blue) surfaces for the **3b** → **4b** and **3a** → **4a** migratory insertions; ΔG and ΔH are in kcal/mol and ΔS is in eu; transition states are in italics.

The favorable $\Delta\Delta G°$ of −2.4 kcal/mol for **4a** formation relative to **4b** is mostly enthalpic in origin, and the $\Delta\Delta H^{\ddagger}$ of −3.5 kcal/mol favoring the ^{neo}Pe-based conversion closely corresponds to the accompanying $\Delta\Delta H°$ of −3.6 kcal/mol. Subtle entropic factors also favor the less rigid ^{neo}Pe system as the change from 4- to 3-coordinate frees up conformational space.

Why does the neopentyl system manifest a greater insertion rate and more favorable thermodynamics? Insight was obtained via BDE and BDFE calculations of the various D(FeR). The favorable thermodynamics for **3a** → **4a** vs **3b** → **4b** tracks with iron-alkyl bond energy differences as the iron(IV) imide converts to the iron(II) amide (Table 2). The iron-alkyl bonds

Table 2. Calculated[a] BDEs and BDFEs for Ground States (GSs) of (Me_2IPr)YFeR ([Fe] = $(Me_2IPr)Fe$)[b]

iron alkyl cmpd	BDE	BDFE
[Fe](^{neo}Pe)$_2$ (**2a**)	51.1	35.5
[Fe](1-nor)$_2$ (**2b**)	57.0	42.2
(AdN=)[Fe](^{neo}Pe)$_2$ (**3a**)	36.5[c]	18.1[c]
	32.3[d]	15.2[d]
(AdN=)[Fe](1-nor)$_2$ (**3b**)	43.5	26.0
	39.5	24.0
{N(Ad)^{neo}Pe}[Fe](^{neo}Pe) (**4a**)	53.8	36.2
{N(Ad)(1-nor)}[Fe](1-nor) (**4b**)	55.5	41.2

[a]B3PW91-GD3/6-31+G(d). [b][Fe] = $(Me_2IPr)Fe$. [c]Triplet GS. [d]Quintet excited state (ES).

exhibit greater changes ($\Delta\Delta H$ = −17.3 vs −12.0 kcal/mol; $\Delta\Delta G$ = −18.1 vs −15.2 kcal/mol) in the ^{neo}Pe system over the 1-norbornyl complexes, despite the latter having larger magnitudes due to the greater s-character of the constrained bridgehead position.

In summary, an increase in covalency enables formally Fe(IV) dialkyl-imides to manifest a rare migratory insertion reaction intrinsic to strong field systems. The chemistry provides hope that $2e^-$ reactivity, such as olefin metathesis, may be possible in formally high oxidation state first-row transition metal systems.

■ ASSOCIATED CONTENT

Supporting Information

The Supporting Information is available free of charge on the ACS Publications website at DOI: 10.1021/jacs.7b06960.

Experimental details on procedures and reactions (PDF)
X-ray crystallographic information pertaining to **1** (CIF)
X-ray crystallographic information pertaining to **2a** (CIF)
X-ray crystallographic information pertaining to **2b** (CIF)
X-ray crystallographic information pertaining to **4a** (CIF)

■ AUTHOR INFORMATION

Corresponding Authors

*ptw2@cornell.edu
*t@unt.edu

ORCID

Peter T. Wolczanski: 0000-0003-4801-0614

Notes

The authors declare no competing financial interest.

DOI: 10.1021/jacs.7b06960
J. Am. Chem. Soc. 2017, 139, 12145−12148

The synthesis and structure of (tmeda)Fe(^{neo}Pe)$_2$ (**1**) have also been done by E. B. Hulley et al. (Univ. Wyoming).

■ ACKNOWLEDGMENTS

We thank the NSF (P.T.W.: CHE-1402149; CHE-1664580. T.R.C.: CHE-1531468), and the DOE (T.R.C.: DE-FG02-03ER15387) for financial support.

■ REFERENCES

(1) (a) Saouma, C. T.; Peters, J. C. *Coord. Chem. Rev.* **2011**, *255*, 920−937. (b) Mehn, M. P.; Peters, J. C. *J. Inorg. Biochem.* **2006**, *100*, 634−643.
(2) (a) Hennessy, E. T.; Liu, R. Y.; Iovan, D. A.; Duncan, R. A.; Betley, T. A. *Chem. Sci.* **2014**, *5*, 1526−1532. (b) Hennessy, E. T.; Betley, T. A. *Science* **2013**, *340*, 591−595. (c) King, E. R.; Hennessy, E. T.; Betley, T. A. *J. Am. Chem. Soc.* **2011**, *133*, 4917−4923. (d) Iovan, D. A.; Betley, T. A. *J. Am. Chem. Soc.* **2016**, *138*, 1983−1993.
(3) (a) Chow, T. W.-S.; Chen, G.-Q.; Liu, Y. G.; Zhou, C.-Y.; Che, C.-M. *Pure Appl. Chem.* **2012**, *84*, 1685−1704. (b) Liu, Y. G.; Guan, X. G.; Wong, E. L. M.; Liu, P.; Huang, J. S.; Che, C.-M. *J. Am. Chem. Soc.* **2013**, *135*, 7194−7204.
(4) Jensen, M. P.; Mehn, M. P.; Que, L. *Angew. Chem., Int. Ed.* **2003**, *42*, 4357−4360.
(5) Paradine, S. M.; White, M. C. *J. Am. Chem. Soc.* **2012**, *134*, 2036−2039.
(6) Cowley, R. E.; Golder, M. R.; Eckert, N. A.; Al-Afyouni, M. H.; Holland, P. L. *Organometallics* **2013**, *32*, 5289−5298. (b) Cowley, R. E.; Holland, P. L. *Inorg. Chem.* **2012**, *51*, 8352−8361.
(7) Gouré, E.; Avenier, F.; Dubourdeaux, P.; Séneque, O.; Albrieux, F.; Lebrun, C.; Clémancey, M.; Maldivi, P.; Latour, J.-M. *Angew. Chem., Int. Ed.* **2014**, *53*, 1580−1584.
(8) (a) Brown, S. D.; Betley, T. A.; Peters, J. C. *J. Am. Chem. Soc.* **2003**, *125*, 322−323. (b) Brown, S. D.; Peters, J. C. *J. Am. Chem. Soc.* **2004**, *126*, 4538−4539. (c) Moret, M.-E.; Peters, J. C. *Angew. Chem., Int. Ed.* **2011**, *50*, 2063−2067. (d) Thomas, C. M.; Mankad, N. P.; Peters, J. C. *J. Am. Chem. Soc.* **2006**, *128*, 4956−4957.
(9) Mehn, M. P.; Brown, S. D.; Jenkins, D. M.; Peters, J. C.; Que, L., Jr. *Inorg. Chem.* **2006**, *45*, 7417−7427.
(10) Ni, C.; Fettinger, J. C.; Long, G. J.; Brynda, M.; Power, P. P. *Chem. Commun.* **2008**, 6045−6047.
(11) (a) Wang, L.; Hu, L.; Zhang, H.; Chen, H.; Deng, L. *J. Am. Chem. Soc.* **2015**, *137*, 14196−14207. (b) Zhang, H. Z.; Ouyang, Z. W.; Liu, Y. S.; Zhang, Q.; Wang, L.; Deng, L. *Angew. Chem., Int. Ed.* **2014**, *53*, 8432−8436.
(12) Nieto, I.; Ding, F.; Bontchev, R. P.; Wang, H.; Smith, J. M. *J. Am. Chem. Soc.* **2008**, *130*, 2716−2717.
(13) Heins, S. P.; Morris, W. D.; Wolczanski, P. T.; Lobkovsky, E. B.; Cundari, T. R. *Angew. Chem., Int. Ed.* **2015**, *54*, 14407−14411.
(14) (a) Bennett, J. L.; Wolczanski, P. T. *J. Am. Chem. Soc.* **1997**, *119*, 10696−10719. (b) Cummins, C. C.; Baxter, S. M.; Wolczanski, P. T. *J. Am. Chem. Soc.* **1988**, *110*, 8731−8733.
(15) (a) Hoyt, H. M.; Michael, F. E.; Bergman, R. G. *J. Am. Chem. Soc.* **2004**, *126*, 1018−1019. (b) Walsh, P. J.; Hollander, F. J.; Bergman, R. G. *J. Am. Chem. Soc.* **1988**, *110*, 8729−8731.
(16) (a) Lindley, B. M.; Swidan, A.; Lobkovsky, E. B.; Wolczanski, P. T.; Adelhardt, M.; Sutter, J.; Meyer, K. *Chem. Sci.* **2015**, *6*, 4730−4736. (b) Lindley, B. M.; Jacobs, B. P.; MacMillan, S. N.; Wolczanski, P. T. *Chem. Commun.* **2016**, *52*, 3891−3894.
(17) (a) Brown, S. N.; Mayer, J. M. *J. Am. Chem. Soc.* **1996**, *118*, 12119−12133. (b) Brown, S. N.; Mayer, J. M. *J. Am. Chem. Soc.* **1994**, *116*, 2219−2220.
(18) Hu, X.; Meyer, K. *J. Am. Chem. Soc.* **2004**, *126*, 16322−16323.
(19) (a) Matsunaga, P. T.; Hess, C. R.; Hillhouse, G. L. *J. Am. Chem. Soc.* **1994**, *116*, 3665−3666. (b) Koo, K.; Hillhouse, G. L. *Organometallics* **1996**, *15*, 2669−2271.
(20) Cenini, S.; Gallo, E.; Caselli, A.; Ragaini, F.; Fantauzzi, S.; Piangiolino, C. *Coord. Chem. Rev.* **2006**, *250*, 1234−1253.
(21) Fürstner, A.; Martin, R.; Krause, H.; Seidel, G.; Goddard, R.; Lehmann, C. W. *J. Am. Chem. Soc.* **2008**, *130*, 8773−8787.
(22) (a) Al-Afyouni, M. H.; Fillman, K. L.; Brennessel, W. W.; Neidig, M. L. *J. Am. Chem. Soc.* **2014**, *136*, 15457−15460. (b) Muñoz, S. B., III; Daifuku, S. L.; Brennessel, W. W.; Neidig, M. L. *J. Am. Chem. Soc.* **2016**, *138*, 7492−7495.
(23) Casitas, A.; Rees, J. A.; Goddard, R.; Bill, E.; DeBeer, S.; Fürstner, A. *Angew. Chem., Int. Ed.* **2017**, *56*, 10108.
(24) (a) Fernández, I.; Trovitch, R. J.; Lobkovsky, E.; Chirik, P. J. *Organometallics* **2008**, *27*, 109−118. (b) Cámpora, J.; Naz, A. M.; Palma, P.; Álvarez, E.; Reyes, M. L. *Organometallics* **2005**, *24*, 4878−4881.
(25) (a) Karsch, H. H. *Chem. Ber.* **1977**, *110*, 2699−2711. (b) Hermes, A. R.; Girolami, G. S. *Organometallics* **1987**, *6*, 763−768.
(26) Xiang, L.; Xiao, J.; Deng, L. *Organometallics* **2011**, *30*, 2018−2025.
(27) Danopoulos, A. A.; Braunstein, P.; Wesolek, M.; Monakhov, K. Y.; Rabu, P.; Robert, V. *Organometallics* **2012**, *31*, 4102−4105.
(28) (a) Katsuki, T. *Chem. Lett.* **2005**, *34*, 1304−1309. (b) Huang, X. Y.; Bergsten, T. M.; Groves, J. T. *J. Am. Chem. Soc.* **2015**, *137*, 5300−5303.
(29) Ryan, S. J.; Schimler, S. D.; Bland, D. C.; Sanford, M. S. *Org. Lett.* **2015**, *17*, 1866−1869.
(30) Byrne, E. K.; Theopold, K. H. *J. Am. Chem. Soc.* **1989**, *111*, 3887−3896.
(31) Bower, B. K.; Tennent, H. G. *J. Am. Chem. Soc.* **1972**, *94*, 2512−2514.
(32) Lewis, R. A.; Smiles, B. E.; Darmon, J. M.; Stieber, S. C. E.; Wu, G.; Hayton, T. W. *Inorg. Chem.* **2013**, *52*, 8218−8227.
(33) (a) Evans, D. F. *J. Chem. Soc.* **1959**, 2003−2005. (b) Schubert, E. M. *J. Chem. Educ.* **1992**, *69*, 62.
(34) Liptrot, D. J.; Guo, J. D.; Nagase, S.; Power, P. P. *Angew. Chem., Int. Ed.* **2016**, *55*, 14766−14769.
(35) Wolczanski, P. T. *Organometallics* **2017**, *36*, 622−631.

DOI: 10.1021/jacs.7b06960
J. Am. Chem. Soc. 2017, 139, 12145−12148